Development of channel waveguide lasers in Nd^{3+}-doped chalcogenide (Ga:La:S) glass through photoinduced material modification

Arshad K. Mairaj, Christos Riziotis, Alain M. Chardon, Peter G.R. Smith, David P. Shepherd and Daniel W. Hewak

Optoelectronics Research Centre, University of Southampton, SO17 1BJ, United Kingdom

We report the development of a waveguide laser source in a neodymium-doped chalcogenide (Ga:La:S) glass. Channel waveguide structures were directly written via above bandgap (λ_{UV}=244nm) illumination provided by a focused UV-laser beam with fluencies 1.5 – 150 J/cm^2. Effects of photoinduced material modification in the form of surface compaction and photodensification were evident. Characterization revealed a low threshold waveguide laser with emission at 1075 nm and slope efficiency of 15 %. The active device was spatially single-mode and exhibited laser operation with 8.6 mW peak power and attenuation < 0.4 dB cm^{-1}.

Integrated optical sources in glass hosts are expected to augment optical processing in glass substrates. It is well known that chalcogenide glasses (ChGs) and amorphous films undergo structural changes when exposed to light. Some of these changes, can be either reversible or irreversible, and have been associated with transformations at the atomic level involving non-radiative recombination of photoinduced electron-hole pairs [1]. The remarkable changes in ChGs when exposed to radiation can potentially provide an interesting route to developing passive and active devices. Direct writing of waveguides with light, either above or below the bandgap of a glassy material has become a topic of great interest [2-3]. Optical interconnects for high data rate systems requiring ultra-fast switching, gas sensors where the absorption bands lie in the near-mid-IR, and systems requiring compact IR laser sources, are just some of the applications where this technology can be utilized [4-6]. Gallium lanthanum sulphide (Ga:La:S) glass is an amorphous semiconductor with bandgap energy of 2.6 eV (475 nm) and a wide transmission window, typically between 0.6-7 μm. The high transition temperature, excellent rare-earth solubility, low-phonon energy, high non-linearity and well documented spectroscopic properties make it an interesting material for planar devices [7]. We have previously demonstrated passive waveguides in Ga:La:S glass through direct-UV writing [8]. In this letter we report, for the first time, active (Nd^{3+}-doped) low-loss channel waveguides in this novel host though direct-UV writing.

Fabrication of Nd^{3+}-Ga:La:S glass, with a typical molar ratio 65 Ga_2S_3 : 31.5 La_2S_3 : 3 La_2O_3 : 0.5 Nd_2S_3, was carried out from prepared batches of powders. These glass precursors were loaded into a vitreous carbon crucible while in a controlled atmosphere. The precursors are non-volatile at the glass melting temperature (1150°C for up to 24h) and were heated in an open (argon purged) atmosphere, after which the melt was quenched and annealed. The bulk glass was cut into slabs (20 x 17 x 2 mm) and polished on the top and bottom faces. After laser writing, the sample was polished at both end faces to allow optical coupling.

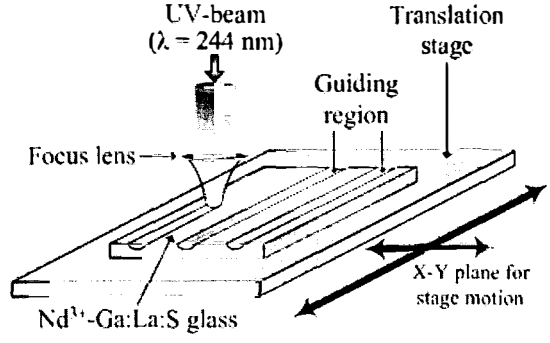

FIG. 1. Schematic diagram of the set-up used to directly write channel waveguides into Nd^{3+}-Ga:La:S bulk glass.

The direct-UV writing set-up shown in Fig. 1 consists of a frequency-doubled UV laser (Coherent FRED Sabre 500) with 200 mW of CW output at 244 nm. A UV grade spherical fused silica lens (35 mm focal length) provides a focused writing spot from the spatially filtered laser beam. The UV beam size is approximately 3.1 mm and the measured spot size of the focused waist ($1/e^2$ radius of intensity) is 3.3 μm. The sample, held in place by a vacuum chuck, was attached to a computer controlled translation stage. The stage, which provided the 2D movement of the sample (X and Y dimensions), has a maximum scan velocity of up to 0.05 m/s and relative position resolution of 0.1 μm. The size of a channel waveguide was determined by both the power density (I_{UV} kW/cm^2) of the focused laser beam and the scan velocity (V_{SCAN} m/s). The average laser fluence (F J/cm^2) applied to the glass surface may then be expressed as [2]:

$$F = \frac{I_{UV} \times a}{V_{SCAN}} \qquad (1)$$

where a is the spot size. For our experiments, the UV spot size was varied between 25 – 50 μm, by varying the

sample to focus distance, providing a power density over the applied area of I_{UV} = 1.5 – 10.2 kW/cm^2. Scan velocity was varied between 0.0017 – 0.05 m/s. Hence, a fluence in the range of 1.5 – 150 J/cm^2 was applied to the glass surface. Micrographs of the channel waveguides were obtained using an analytical scanning electron microscope (SEM, JEOL 6400) to which an energy dispersive X-ray microscope (EDAX), allowing compositional analysis, was attached. The micrograph shown in Fig. 2 is the end-face view of a Nd^{3+}-Ga:La:S sample after direct-UV writing. The channel waveguide shown was written with laser fluence of 10.8 J/cm^2. Photostructural change in the form of surface compaction (1.2 μm) clearly shows the region of index change with physical channel dimensions of 13 μm by 5.5 μm. Measurements within the photomodified region revealed variations in elemental ratios, with an increase in lanthanum content and decrease in gallium and sulphur. Compositional analysis (EDAX) of the waveguide core (exposed region) for channels exposed to 4.5 J/cm^2, 7.2 J/cm^2 and 10.8 J/cm^2 of laser energy revealed lanthanum content to be 57.2 wt%, 65.7 wt% and 67.6 wt% respectively (atomic weight %). Measurements of the unexposed region showed lanthanum content to be 50.2 wt%. This chemical change contributes to the effects of photodensification creating a region of raised refractive index, which is the waveguide core. Variation in applied laser fluence allowed a range of different channels to be fabricated with maximum measured index change ($+\Delta n$) of 10^{-3}.

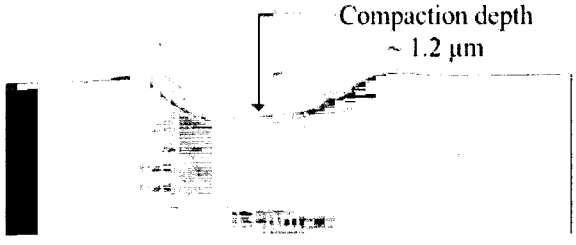

FIG. 2. Micrograph (SEM) of a typical channel waveguide written with laser fluence 10.8 J/cm^2 shows surface compaction of 1.2 μm with physical channel size 13 μm by 5.5 μm.

The Ga:La:S glassy composition has previously been investigated by extended X-ray absorption fine structure (EXAFS, gallium K-edge, lanthanum LIII edge) spectroscopy. The structural model proposed for this glass type is the modified random network, which is similar to that for glasses from the oxide family such as sodium silicate. This proposed model, although disordered, is a well-defined environment with a covalent network of GaS_4 tetrahedra intercalated by the essentially ionic La-S channels [9]. Most binary ChGs such as As_2S_3, As_2Se_3 and GeS_2 exhibit fractional volume expansion (+ $\Delta V/V$) upon light illumination. This volume expansion is understood to be related to point defects in the glass structure. In contrast irradiation of oxide glasses such as SiO_2, with its disordered three-dimensional random network structure, gives rise to the opposite effect leading to radiation compaction (- $\Delta V/V$) with photodensification [10]. In the case of $GeAs_4Se_5$, a ternary non-stoichiometric ChG, the structure is assumed to be fairly random and three-dimensional and as such does exhibit radiation compaction as was observed in SiO_2 glass [11]. In any case, diffraction pattern studies for both oxide and ChGs have shown similar results; irradiation seems always to enhance the randomness of an amorphous structure.

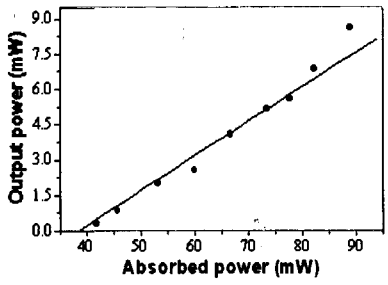

FIG. 3. Peak output power of 8.6 mW for 89 mW of absorbed pump power and slope efficiency of 15 % with the upper limit of waveguide attenuation < 0.4 dB cm^{-1}.

The channel waveguide characterized for laser performance was written with I_{UV} = 10.2 kW/cm^2 and V_{SCAN} = 0.04 m/s giving an applied fluence of 6.1 J/cm^2. The lasing characteristics were tested using the 1075 nm $^4F_{3/2} \rightarrow {}^4I_{11/2}$ transition of Nd^{3+}-Ga:La:S. The investigated sample had a concentration of 0.7 mol% Nd_2S_3 and a length of 16 mm. Laser light from a tunable Ti:sapphire was coupled into the waveguide using a single launch X 6.3 microscope objective. Guided light from the waveguide was collected with a X 10 microscope objective and directed through an iris to isolate light from the guided mode of the waveguide from that of the substrate. Optimization of launch efficiency was performed with the aid of a CCD camera, allowing observation of the channel mode, as well as through fluorescence intensity measurements. A launch efficiency of 30 % was calculated from transmission measurements with the Ti:sapphire tuned off the Nd^{3+} absorption band. The rather low value for the launch efficiency was possibly due to the mismatch between the launched pump beam profile and the guided pump mode profile in the waveguide. In order to form the laser cavity, lightweight thin mirrors were butted to the end-faces of the guide, using a thin film of fluorinated liquid for adherence. The input mirror (R_1) was 98 % reflective at the lasing wavelength (1075 nm) and had 87 % transmission at the pump wavelength (815 nm). Three sets of output mirrors with different reflectivities (R_2) were utilized with 2 %, 8 % and 12.5 % transmission at the signal wavelength. Lasing threshold was noted for each case. With the 2 % output coupler, the threshold was as low as 15.1 mW of absorbed pump power, and increased to 18.7 mW with the 8 % output coupler. With the 12.5 % output coupler the threshold rose to 33.8 mW with laser output results shown in Fig. 3. An output slope efficiency of 15 % with respect

to absorbed power was obtained, with an output power of 8.6 mW for the maximum available 89 mW of absorbed power. Measurement of the laser output with a spectrum analyzer (ANDO) revealed a lasing wavelength of 1075 nm. This is at the same wavelength at which the fluorescence emission spectrum has maximum intensity and corresponds to the wavelength of maximum internal material gain. Observation and measurements of the pump and lasing mode were performed with a CCD camera, and it was observed that both the pump and laser output modes were in fundamental spatial-mode. Modal dimensions ($1/e^2$ radius of intensity) were W_{px} = 4.2 μm by W_{py} = 3.3 μm for the pump mode, and W_{lx} = 4.4 μm by W_{ly} = 5.7 μm for the laser mode. Observation of the laser emission from the output of the waveguide indicates that the guided beam was approximately Gaussian. Evaluation of attenuation in the laser device was estimated first by the Findlay-Clay method [12]. For a four-level waveguide laser system with negligible depopulation of the ground state, the absorbed launched pump power at threshold $P_{th\ abs}$ can be expressed as:

$$P_{thabs} = K\left(2\alpha\ell - \ln(R_1R_2)\right) \qquad (2)$$

where K is a constant dependent upon the material parameters, the quantum efficiency and the pump and signal spatial properties, α is the waveguide propagation attenuation coefficient, ℓ is the device length and R_1 and R_2 are the reflectivities of the input and output mirrors at the laser wavelength. A plot of $P_{th\ abs}/\ell$ versus $-\ln(R_1R_2)/2\ell$ is shown in Fig. 4. The intercept on the x-axis is indicative of the propagation attenuation coefficient in the laser cavity and gives an approximate value of α = 3 m^{-1}. The attenuation in the cavity due to the waveguide can then be calculated to be ~ 0.2 dB cm^{-1}. Due to the lack of output couplers with higher transmission at the signal wavelength, this attenuation figure was confirmed with a separate calculation involving the slope efficiency (η) using the relation [13]:

$$\eta = \eta_q \cdot \frac{\nu_l}{\nu_p} \cdot \frac{T}{T+L} \cdot \frac{W_{lx}W_{ly}(2W_{px}^2 + W_{lx}^2)^{1/2}(2W_{py}^2 + W_{ly}^2)^{1/2}}{(W_{px}^2 + W_{lx}^2)(W_{py}^2 + W_{ly}^2)} \qquad (3)$$

where η_q is quantum efficiency of the device (assumed to be 100%), ν_l and ν_p are the laser and pump frequencies, T is the output coupler transmission at the laser wavelength, L is the roundtrip internal loss, W_{lx}, W_{ly}, W_{px} and W_{py} refer to the $1/e^2$ intensity radii for the laser and pump modes in the horizontal and vertical planes respectively. Assuming all the loss is due to the waveguide attenuation, we find an upper limit for the propagation loss of < 0.4 dB cm^{-1} as calculated from equation (3) for η = 15% and T = 12.5%. This attenuation figure is comparable to values quoted in our previous work in direct-UV written passive waveguides [8], and is consistent with the Findlay-Clay analysis.

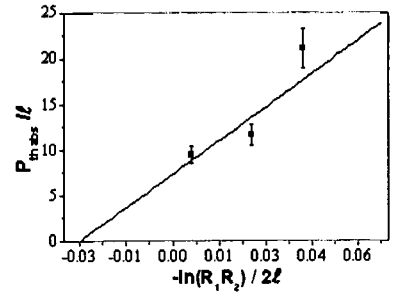

FIG. 4. Plot of $P_{th\ abs}/\ell$ against $-\ln(R_1R_2)/2\ell$ where intercept with x-axis gives waveguide propagation attenuation coefficient α = 3 m^{-1}.

In summary, we have shown that photoinduced changes can be introduced by directly writing waveguides into Nd^{3+}-Ga:La:S glass through exposure to short wavelength light (λ = 244 nm). The development of an active device in Nd^{3+}-Ga:La:S glass has yielded single-mode channel waveguides. Maximum laser output (λ = 1075 nm) of 8.6 mW for an absorbed laser pump power of 89 mW and slope efficiency of 15 % was achieved with attenuation in this device measured to be < 0.4 dB cm^{-1}. It is expected that by directly coating mirrors onto the waveguide ends, thereby reducing coupling losses, higher slope efficiencies may be achieved. This initial demonstration suggests that further optimization of glass quality and direct writing conditions could lead to efficient low-loss channel waveguide devices for use with integrated optics. In particular, the potential for developing laser waveguides with emission in the mid-IR such as erbium-doped devices seems promising.

This work was supported in part by a DTI/EPSRC grant through the LINK Photonics Programme, funding from Pirelli Cavi and by EPSRC grant GR/N09787.

[1] K. Tanaka, Current Opinion in Solid State & Materials Science **1**, 567 (1996).
[2] M. Svalgaard, C.V. Poulsen. A. Bjarklev and O. Poulsen, Electron. Lett. **30**, 1401 (1994).
[3] O.M. Efimov, L.B. Glebov, K.A. Richardson, E. Van Stryland, T. Cardinal, S.H. Park, M. Couzi and J.L. Bruneel, Opt. Materials **17**, 379 (2001).
[4] J. Lucas, Current Opinion in Solid State & Materials Science **4**, 181 (1999).
[5] C. Gmachl, H.Y. Hwang, R. Paiella, D.L. Sivco, J.N. Baillargeon, F. Capasso and A.Y. Cho, IEEE Photon. Technol. Lett. **13**, 182 (2001).
[6] A. Saliminia, A. Villeneuve, T.V. Galstyan, S. LaRochelle and K. Richardson, J. Lightwave Technol. **17**, 837 (1999).
[7] Y.D. West, T. Schweizer, D.J. Brady and D.W. Hewak, Fibre Integrated Opt. **19**, 229 (2000).
[8] A.K. Mairaj, A. Fu, H.N. Rutt and D.W. Hewak, Electron. Lett. **37**, 1160 (2001)
[9] S. Benazeth, M.H. Tuilier, A.M. Loireau-Lozac'H, H.Dexpert, P.Lagarde and J.Flahaut, J. Non-Cryst. Sol. **110**, 89 (1989).
[10] A.R. Silin, J. Non-Cryst. Sol. **129**, 40 (1991).
[11] H. Hamanaka, K. Tanaka, A. Matsuda and S. Iizima, Solid State Comms. **19**, 499 (1976).
[12] D. Findlay and R.A. Clay, Phys. Lett. **20**, 277 (1966).
[13] W.A. Clarkson and D.C. Hanna, J. Mod. Opt. **36**, 483 (1989).